

Copyright © 2009 Year IEEE. Reprinted from IEEE TRANSACTIONS ON ADVANCED PACKAGING. Such permission of the IEEE does not in any way imply IEEE endorsement of any of Institute of Microelectronics' products or services. Internal of personal use of this material is permitted. However, permission to reprint/republish this material for advertising or promotional purposes or for creating new collective works for resale or redistribution must be obtained from the IEEE by writing to pubs-permission@ieee.org.

Development of Optical MUX/DEMUX on Silicon Optical Bench—Assembly Accuracies

Chee-Wei Tan, Teck-Guan Lim, Jing Li, Tangdionga Geri Endrio, Yi-Yoon Chai, Seiji Maruo, Pamidighantam V. Ramana, Seung-Wook Yoon, *Member, IEEE*, and John H. Lau, *Fellow, IEEE*

Abstract—An optical subassembly of MUX/DEMUX where optical devices are hybrid-integrated on a silicon optical bench (SiOB) using a passive alignment method is reported. A tight tolerance of positional and tilting angular accuracy is required for optical devices attachment in order to maximize the coupling efficiency. The critical positioning transverse to the optical axis merely depends on the symmetry, and accuracy of the position and shape of trenches. Any inaccuracy primarily affects the noncritical positioning, i.e., z -axis and θ_z , in the direction along the optical axis; misalignment accumulated and causes undesired insertion loss. All the piece parts, i.e., mirror, thin-film filters (TFFs), ball lens, SiOB, etc., have a defined tolerance in their dimensions and surfaces which increases the challenge in achieving high placement accuracy along the optical axis. The effects from these inherent inaccuracies of the position and shape of trenches and piece parts could be minimized by optimizing the adhesive volume, improve the bottom flatness, proper procedure selection. Misalignment at each axis, e.g., x -, y -, z -, θ_x , θ_y , and θ_z was characterized and its effect to the coupling efficiency was discussed.

Index Terms—Accuracy, adhesive, coupling efficiency, passive alignment, silicon optical bench.

I. INTRODUCTION

THE assembly of transceiver package required multiple active alignment steps of bulk optic discrete subcomponents which is a costly and time consuming procedure. There has been increasing demand in manufacturing the low cost optical modules where most of the structures employed optical subassemblies (OSAs) to package the optoelectronic devices and optic components in a module [1], [2]. Out of the many alternatives, Hewlett Packard's SpectraLAN project had reported a DEMUX was generated for the CWDM module of a small form factor transceiver [3], [4]. HP approach was to use polymer waveguide for the DEMUX [10], while, silicon optical bench (SiOB) is utilized as a platform to integrate optical components and subsystems in this study.

Manuscript received December 26, 2007; revised June 18, 2008; May 07, 2009. Current version published August 05, 2009. This work was recommended for publication by Associate Editor A. Shapiro upon evaluation of the reviewers comments.

C.-W. Tan, T.-G. Lim, J. Li, T. G. Endrio, Y.-Y. Chai, P. V. Ramana, S.-W. Yoon, and J. H. Lau are with Institute of Microelectronics, A*STAR (Agency for Science, Technology and Research), Singapore 117685 (e-mail: tancw@ime.a-star.edu.sg; limtg@ime.a-star.edu.sg; lij@ime.a-star.edu.sg; tangdionga@ime.a-star.edu.sg; chaiyy@ime.a-star.edu.sg; pvrmana@ime.a-star.edu.sg; yoonsw@ime.a-star.edu.sg; lauhs@ime.a-star.edu.sg).

S. Maruo is with Hitachi Cable, Ltd., Tokyo 101-8971, Japan (e-mail: maruo.seiji@hitachi-cable.co.jp).

Color versions of one or more of the figures in this paper are available online at <http://ieeexplore.ieee.org>.

Digital Object Identifier 10.1109/TADVP.2009.2024693

The SiOB technology enables the automation of fiber optic components packaging and the integration of multiple functions onto a single silicon platform using simple mechanical positioning to form passive optical alignment. This provides the potential of realizing miniature multichannel transmitter optical subassembly (TOSA) and receiver optical subassembly (ROSA) without using expensive active alignment equipment and process. Other advantages of SiOB technology include scalable production, lower per unit manufacturing costs, versatility for integrating into existing product platforms and enhanced testing and measurement capabilities. Despite these advantages, there are a few critical challenges, such as sub-micron fabrication accuracies and submicron post bonding accuracy.

The use of silicon optical bench for optical hybrid integration has been widely reported and discussed [5]–[9]. Li *et al.* used silicon on insulator (SOI) wafer for making the SiOB [9]. Dautartas *et al.* believed that SiOB technology as a platform can meet the needs of the datacom sector, i.e., high performance, and low cost [10]. They had demonstrated this platform as a very robust technology in the telecom sector and have greatly reduced the cost of ownership lending itself to low cost, high volume manufacturing [11], [12]. Boudreau *et al.* [12] had reported a passive alignment approach to precisely place the active devices onto the SiOB.

This paper is part of the project to develop a prototype hybrid package, an ultra-miniature four channels TOSA/ROSA for CWDM applications, and to report on the tolerance analysis for passive alignment. The objective of this project is to develop an ultra-miniature of 5 mm × 10 mm × 6 mm four channels transmitter (Tx) and receiver (Rx) optical subassembly (OSA). The small size is to be realized mainly through IME Silicon Optical Bench Technology with commercial available thin film filters (TFFs) and micro mirrors. The work includes optical simulation and optimization of all the channels with single mode fiber, fabrication and assembly of the OSA. The test vehicle for this paper is optical subassembly of DEMUX on SiOB which is purely optics.

II. EXPERIMENTAL METHODOLOGY

Fig. 1 shows the basic fabrication process of Silicon Optical Bench. It started with 1 μm SiO₂ deposition on the silicon substrate playing the role of hard mask as show in Fig. 1(a). Then, dry film was laminated onto the substrate and the trenches were patterned by using 1 to 1 photolithography as seen in Fig. 1(b). In order to expose the silicon, the hard mask SiO₂ was etched [Fig. 1(c)], STS deep reactive ion etching (DRIE) was then carried out [Fig. 1(d)] and followed by photoresist strip [Fig. 1(e)]. In fabrication, the trench size was made slightly larger to make

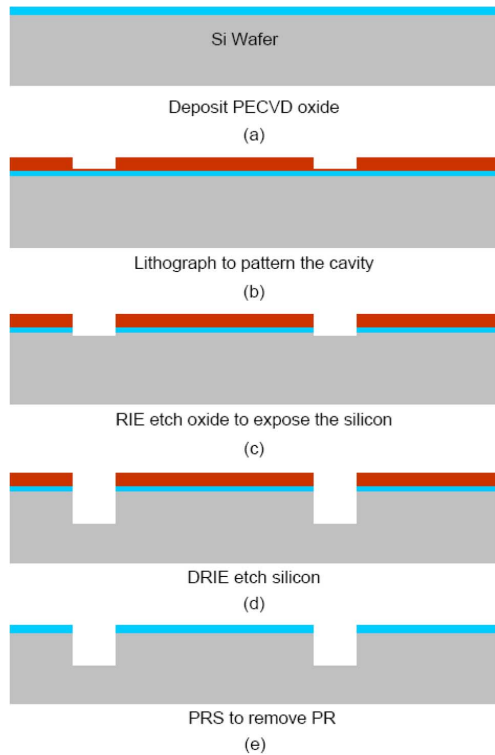


Fig. 1. Fabrication process for SiOB.

TABLE I
DIMENSION FOR DEVICES AND CAVITIES ON SiOB
(ALL DIMENSIONS IN MILLIMETERS)

	Ball lenses	TFF	Mirror
Physical Dimension	0.500± 0.003	H0.3±0.02 ×W0.8±0.05 ×D0.5±0.01	H1.0 ×W1.5 ×D0.5
Cavity	0.50 0.51 0.52	0.32 × 0.51 0.33 × 0.53 0.34 × 0.54	1.50 × 0.50 1.52 × 0.52

sure the devices can go in without failure. TFFs and mirrors were assembled into trenches with different tolerance as listed in Table I to determine the suitable size.

A simple comparison study on the effect of adhesive volume was carried out to further improve the perpendicularity of the adhered optical devices, i.e., TFFs and mirror. Then, these data was utilized to improve the coupling efficiency of SiOB. In the meantime, three methods for TFF attachment were carried out on larger trench: free placing, adjusted the TFF to as center as possible, and push the TFF as close as possible to the side wall. These materials were then cross-sectioned and then inspected using scanning electron microscope (SEM). Tilting angle, θ_x for these samples were determined using Wyko interferometer, HD 3300 and image processing software.

Throughout this paper, simulation data was used for reference. Simulation software, ASAP from Breault Research Organization was used to determine the coupling efficiency (η) of this DEMUX assembly. The effect of ball lenses shift from the optical axis was simulated and discussed. Fig. 2 shows the plane view of SiOB layout and the definition of each axis. One DEMUX on SiOB was assembled, and its coupling loss at each channel was measured using Suruga Seiki's automated fiber

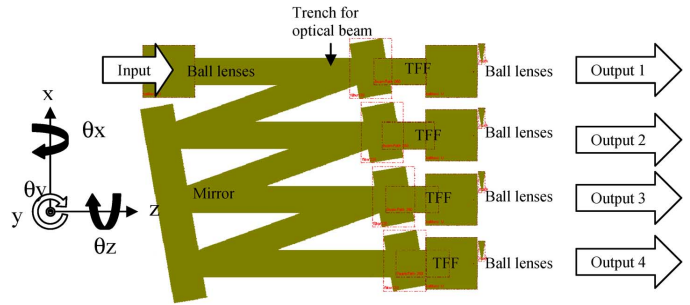


Fig. 2. Plane view of the SiOB with definition for axes.

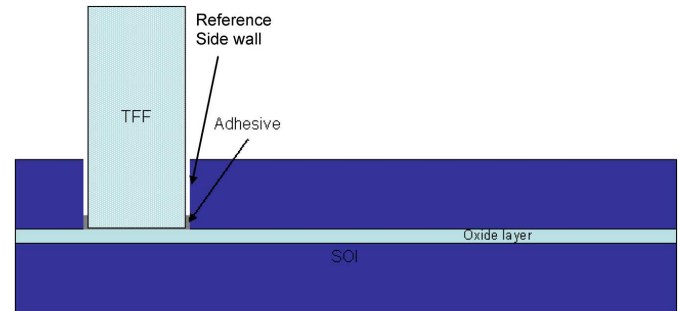


Fig. 3. Schematic of TFFs assembled onto SOI SiOB.

alignment system consists of six axes motion with a resolution of 25 nm.

Silicon on insulator (SOI) wafers were used to avoid the issue of different y -depth along the optical path and to ensure it is co-axial with a tolerance of $< \pm 1 \mu\text{m}$. Mirrors and Mirrors 1 ~ 3 with known perpendicularity were used to verify the effectiveness of the optical design regardless of the inherited inaccuracies of optical devices, as shown in Fig. 3. These specially made Mirrors 1 ~ 3 were used to replace the filter and placed in the SiOB without adhesive bonding. Coupling power was measured using SMF and MMF after the output ball lenses, which started with Channel 4. Then, Mirror 3 was removed, the fibers and output ball lens was shifted to channel 3. These steps were repeated for Channel 1 and 2. These measured coupling losses were then compared to the simulation data.

III. RESULTS AND DISCUSSION

The SiOB and optical devices with the dimension as listed in Table I, were used for evaluation. A few potential contributors to the coupling loss are discussed in the following. Results show that the trench dimension has to be slightly larger than the actual optical devices, in order to accommodate the tolerance of the optical devices. Too large of trench dimension may lead to increase in variation in θ_y -axis for TFFs and mirrors which will cause the incident beam mis-hit in x -direction. Besides the inconsistent Y -depth, the width of the trenches in x -axis will also affect the ball lenses concentric along the optical axis. In this case, the selected cavity sizes for the following experiments are: 0.5 mm for ball lens, 0.32×0.51 for TFF and 1.5×1.5 mm for mirror, respectively.

Fig. 4 shows the cross-sectioning view of two mirrors assembled using huge amount of adhesive [Fig. 4(a)] and lesser amount of adhesive [Fig. 4(b)], respectively. The tilting angle, θ_x obtained are 1.1° and -1.0° , respectively. The tilting angle

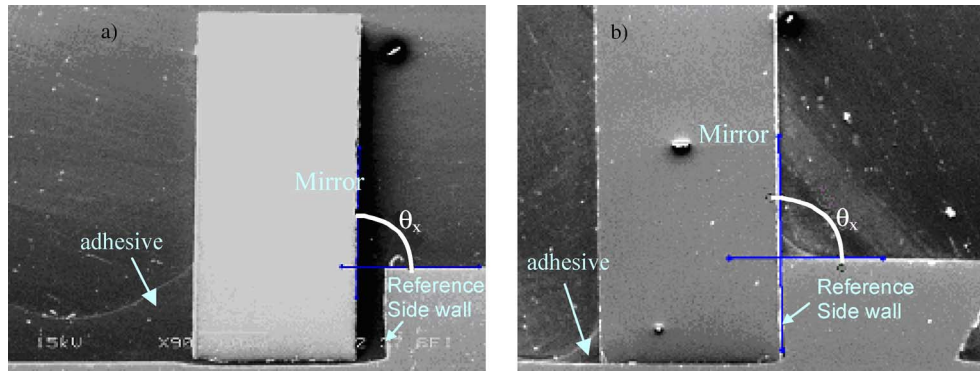


Fig. 4. Cross-sectioning view mirror assembled using (a) huge amount of adhesive and (b) less amount of adhesive.

TABLE II
TILTED ANGLE OF MIRROR IN θ_x DIRECTION

Conditions	Tilted Angle, θ_x ($^\circ$)			
	1	2	3	Average
A (push to side wall)	-0.7	-0.9	-0.8	-0.8
B (Center)	0.8	1.0	3.4	1.7
C (free placing)	-0.9	1.0	1.3	0.5

was minimized to -0.7° when minimum adhesive was applied on the bottom of the trench.

Mirrors were attached into the SiOB trenches using three different positioning approaches as listed in Table II for comparison. Though free placing of mirror results in only 0.5° offset from 90° in average, it is inconsistent. When mirror was placed in the center of a larger trench resulted in most inconsistent tilted angle, θ_x . This is because tilted mirror or TFF will reflect the laser beam upwards or downwards depends on the direction of the θ_x . Therefore, by pushing the mirror as close as possible to the cavity side wall at the direction of the incident beam resulted in most consistent tilted angle, which is -0.8° and most preferred among these three approaches.

By measurement using interferometer, it was found that the optical devices that consist of inherited dimension error have contributed to the tilting angle as well. TFFs and mirrors were singulated by dicing process with an uncontrolled dicing edge, it is known that these edges will not be perfectly 90° , and flat. These dicing edges will contact directly to the bottom surface of the trenches results in a random tilted angle in term of direction and magnitude. The contribution of this factor to θ_x was determined to be around $-0.7 \sim -1.0^\circ$.

Beside the dummy TFFs' and mirror's tilt angle, the positions of the ball lenses are also a major source of the optical coupling loss. For the ball lens assembly, it is crucial to align all the four output ball lenses with respect to the input ball lens, which determine the optical path. However, unlike the dummy TFFs, the optical misalignment of the output ball lens does not have a cumulative effect on the subsequent channels. Fig. 5 shows the modeled coupling losses when input and output ball lenses were shifted off the best position in x -axis. Obviously, misalignment of output ball lens has more effect to coupling loss, i.e., $4 \sim 5 \mu\text{m}$ shift contributed to about 4 dB loss.

It is hardly to obtain a perfectly flat bottom surface of the etched trench; a curve bottom surface was shown in Fig. 4. This will contribute to different in y -depth along the optical path, and

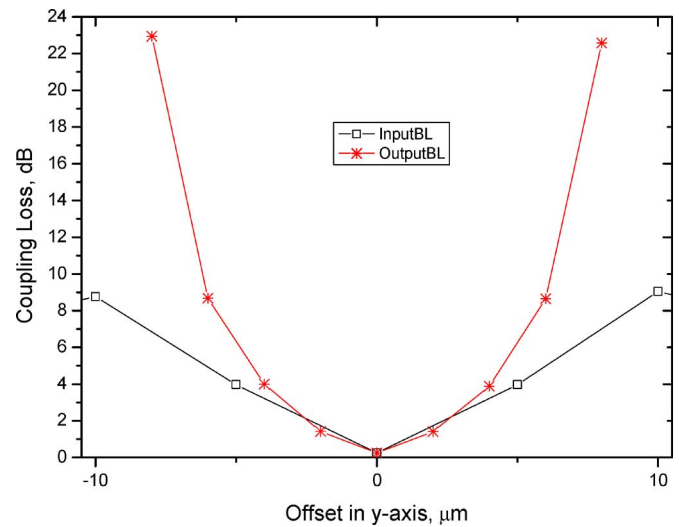


Fig. 5. ASAP simulation result of DEMUX on SiOB.

this is especially critical for ball lenses. Inconsistent y -depth is not so critical for mirror and TFFs, however, curvature in the bottom surface may contribute to larger tilting angle, θ_x . This could be solved by using V-groove; however, due to complication in fabrication, SOI wafer was used to provide a flat surface at the bottom in the later experiments to reduce the error in y -axis. It is expected that with SOI wafer, the cavity depth for all the ball lens cavities will be constant. Thus, all the input and output ball lenses when placed in the SiOB will be in co-axial at y -axis. Therefore, misalignment in the y -axis will be minimized.

A. Test Structures Using SOI Wafer

Fig. 6 shows the design of the DEMUX on SiOB made of SOI wafer which consists of five $500 \mu\text{m}$ diameter BK7 ball lens, four TFFs with different operating wavelength, and a mirror. For ideal condition, the simulated coupling losses for this design using single mode fiber (SMF) as input and output collector for all the channels are shown in Table III. The insertion losses of the optical components are not included in the simulations. The higher loss at channel 4 is due to the dispersion effect of the optical beam, which increases as the optical path length increases. Table III also shows the measured coupling loss of an assembled DEMUX where SMF is used at input to deliver laser beam at a particular wavelength, and at output to collect optical signal. For this measurement, the operating wavelengths

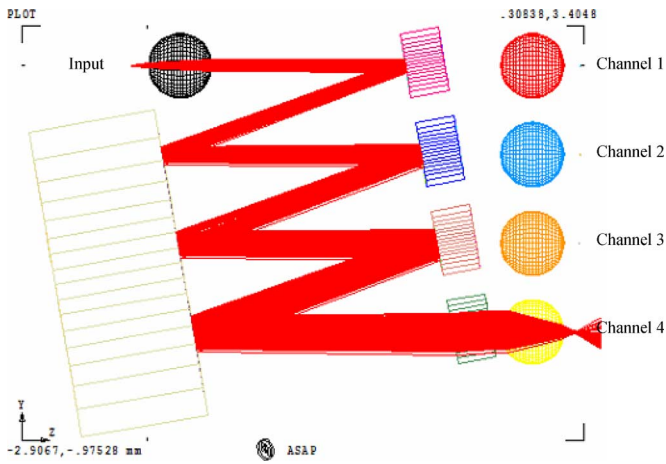


Fig. 6. Losses due to ball lenses shift.

TABLE III
MEASURED COUPLING LOSS OF THE ASSEMBLED DEMUX

Channel	Simulation Loss, dB	Loss, dB	
		SMF-SMF	SMF-MMF
1	~0.00	4.0	1.3
2	0.06	11.5	2.6
3	0.32	16.1	6.8
4	1.32	20.3	8.7

for channel 1, 2, 3, and 4 are set to 1275 nm, 1300 nm, 1325 nm, and 1350 nm, respectively. A wideband tunable laser is used as the optical source. For each wavelength measurements, the optical power is first measured and used as a reference input power for the respective channel. The ball lenses, TFFs and mirror are assembled to the SiOB using epoxy. The input and output fibers are not assembled permanently on the SiOB, their positions are allowed to be optimized through active alignment during the measurement. In general, the coupling loss increases as the channel number increases. The losses are mainly due to the misalignments of the TFFs and the mirror, which have accumulative effects, causing a highest loss on the last channel. Hence, in order to maintain good overall performance, mainly determined by Channel 4, the input fiber should align and fix its position to the output fiber at Channel 4. Another measurement is carried out for this test structure using a MMF with core diameter of $62.5 \mu\text{m}$ to couple the output optical signal. Similarly the losses increase as the channel number increases. However, due to the larger core diameter of the MMF, the results as shown in Table III have a much lower coupling loss. Higher optical power loss was observed for this assembly if compares to the modeling data.

A test structure is redesigned with the dummy TFFs (mirrors 1–3) and mirror, which has the same dimension but with controlled sidewall perpendicularity. The dummy TFFs are mirrors, which do not have the function of the filter in the pass band. They are used to simulate the out of band function, which will reflect the optical signal at the design incidence angle of 10° . The dimension of mirrors is of $0.794 \pm 0.002 \times 0.305 \pm 0.002 \times 1.905 \pm 0.002$ mm with an angle, $\theta_x = 90.38^\circ$. While the dimension of the dummy TFFs is of $0.795 \pm 0.005 \times 0.305 \pm 0.002 \times 0.505 \pm 0.005$ mm, with an angle, $\theta_x = 89.37^\circ$. Mirrors with

known perpendicularity were used to verify and determine the contribution of inherent inaccuracies of the optical devices to the coupling loss.

Table IV shows the simulated coupling loss at channel 4 for dummy TFFs and mirror under various titling combinations in θ_x direction. The result also shows that the maximum coupling loss is infinity. As there is an additional dummy TFF in the design and the propagating distance is longer, there are more combinations that resulted in infinity coupling loss. For channel 4, the best result is not obtained when the dummy TFFs have the same tilting angle direction and is opposite to the mirror. Instead, the best coupling loss of ~ 6 dB is obtained when dummy TFF1 and the mirror have opposite tilting direction, and the dummy TFF1 and TFF2 have opposite tilting direction, as highlighted in Table IV. Unlike the results given in channel 2 and channel 3 simulations, the tilting of the optical components in the same direction help to compensate the misalignment angle and give the best result. This is because the titling angle of the dummy TFF and the mirror are not the same, and with a longer optical propagating distance and an additional dummy TFF for channel 4, over compensation occurs. The above results demonstrated that there are optimal orientations of the optical components for the given titling angle for different channels. Hence, the performances of the various channels have to be compromised. In the practical situation where the optical components are assembled, all the dummy TFFs will mostly be titling in the same direction as they have the same perpendicularity angle vector, and hence the loss of the channel 4 will be high, over 20 dB as shown in the simulation results in Table IV. This loss will increase significantly if the mirror tilt angle is opposite to what is desired.

Fig. 7 shows the top view of the assembled SiOB made of SOI wafer, with Mirror, Mirror 1–3 (Dummy TFFs) and ball lenses. Again, SMF was used for input laser beam, while MMF and SMF were used as output collector for comparison. The optical power is first measured and used as a reference input power for the respective channel. The measurement of a particular channel will be done with the respective channel dummy TFF removed so that the optical signal can be coupled to the respective channel's ball lens and output fiber. Hence all the optical components are placed into their respective cavities without permanently fixing. Table V shows the coupling losses obtained by MMF and SMF which has a core size of $62.5 \mu\text{m}$ and $9 \mu\text{m}$, respectively. It shows that the optical power travel along the optical path with certain loss before reaching the detector, MMF and SMF in this case.

Table V also shows the simulation data with consideration of the known tilted angle in θ_x contributed by mirrors when SMF is used as collector. It was found that the measured coupling loss is higher than the simulation data, and is increasing with the channel number increase. Most probably, there is misalignment in x - and y -axis cumulated along the path that caused the beam misaligned to the output fibers. However, the maximum coupling loss obtained for this set up is ~ 16 dB at Channel 4, much lower than the ~ 25 dB obtained for the actual TFF test structure. Assuming the components losses for both test structures are the same, the improved loss is due to the better component sidewall perpendicularity, which reduces the degree of misalignment. The optimizing procedure also helps to reduce the coupling loss, which allows additional alignment of the TFFs,

TABLE IV
EFFECTS OF DIRECTION OF TILTED ANGLE, θ_x TO COUPLING LOSS AT CHANNEL 4

Tilting Big Mirror [degree]	Tilting Mirror1 [degree]	Tilting Mirror2 [degree]	Tilting Mirror3 [degree]	Loss [dB]
0	0	0	0	1.3
-0.38	0.63	0.63	0.63	∞
-0.38	0.63	0.63	-0.63	∞
-0.38	0.63	-0.63	0.63	∞
-0.38	0.63	-0.63	-0.63	11.2
-0.38	-0.63	0.63	0.63	18.2
-0.38	-0.63	0.63	-0.63	6.3
-0.38	-0.63	-0.63	0.63	∞
-0.38	-0.63	-0.63	-0.63	21.7
0.38	0.63	0.63	0.63	21.6
0.38	0.63	0.63	-0.63	∞
0.38	0.63	-0.63	0.63	6.3
0.38	0.63	-0.63	-0.63	18.5
0.38	-0.63	0.63	0.63	11.2
0.38	-0.63	0.63	-0.63	∞
0.38	-0.63	-0.63	0.63	∞
0.38	-0.63	-0.63	-0.63	∞

* ∞ —indicates that the light fall out side of the core hence can not be captured by SMF

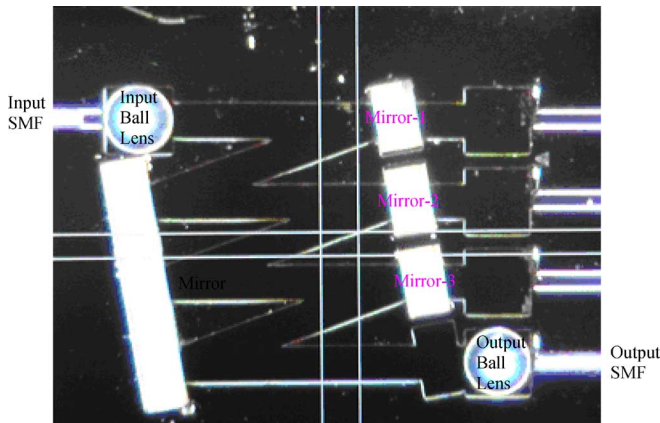


Fig. 7. Top view of the test structure with fibers, ball lenses, and mirrors.

TABLE V
MEASURED COUPLING LOSS OF TEST STRUCTURE

Channel	Coupling Loss, dB		
	Simulation (SMF-SMF)	SMF-SMF	SMF-MMF
1	-	3.1	1.2
2	0.9	7.3	2.8
3	6.3	11.7	6.0
4	21.7	16.1	8.1

mirror, and ball lenses. Furthermore, the measured loss difference between each channel was lower than the simulated result. This could be due to compensation happened when the mirrors were pushed to the side wall of the trenches that reduce the actual θ_x along the optical path.

Another measurement carries out for this test structure using a MMF to couple the output optical signal, also shows that the loss increases as the channel number increases. The performance of the MMF output coupling is much better than the SMF output coupling as the MMF has a very much larger core diameter of $62.5 \mu\text{m}$ as compared with the SMF core diameter of $8.2 \mu\text{m}$

(~ 8 dB versus ~ 16 dB). The coupling loss obtained for this set up is also better than that obtained for the actual TFF test structure (~ 8 dB versus ~ 9 dB). The majority of the coupling loss is probably due to propagation loss, reflection loss at each interface, and excessive beam diameter where part of the beam was blocked by the optical trench. The use of SOI wafer might has taken out the effect of poor surface flatness, the ball lenses which is held by a flat groove instead of V-groove could be still subjected to misalignment of a few microns in x-axis.

Then, this knowledge was used to assemble a DEMUX on a SiOB made of SOI wafer. Fig. 8 shows the cross-sectional view of the mirror assembly on a SiOB made of SOI wafer. Two assembled samples, sample A and B with known θ_x (89.37° and 90.07°) were cross-sectioned. The additional tilting angle or error (E) induced by the assembly are $+0.25^\circ$ and -0.36° for Sample A and Sample B, respectively. The positive sign meant that epoxy assembly has caused the Sample A to tilt forward (left), while Sample B to tilt backward (right). Hence, Sample A verticality has been improved from 89.37° to 89.62° (0.38° from verticality) while Sample B has been over compensated from 90.07° to 89.71° (0.29° from verticality).

An alternative solution is to utilize the hybrid glass submount SiOB structure as proposed during the development. The glass submount with one surface is coated to form a mirror and the opposite surface is used to assemble the TFF perpendicularly, while the SiOB is used to provide the ball lens assembly accuracy, as shown in Fig. 9. Preliminary simulation results show that the insertion loss of <0.3 dB is allowed for a tolerance of $\pm 1^\circ$ in the direction of θ_x . The idea is to make use of the relatively consistent wafer surface condition which is usually formed by precision machining, and the high precision attachment scheme to minimize the tilting angle misorientation, θ_x , to be less than $\pm 1^\circ$. As mirror is also attached to the same glass block, the accumulated tilting angle will be lesser if compare to free space assembly. In addition, the required PD and the laser diode can also be integrated on the SiOB directly, and simplify the assembly process.

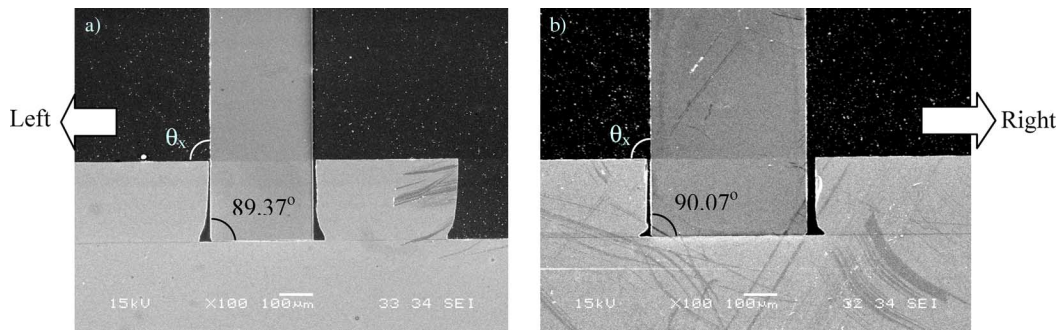


Fig. 8. Cross section view of a mirror assembly on SiOB made of SOI wafer (a) sample A and (b) sample B.

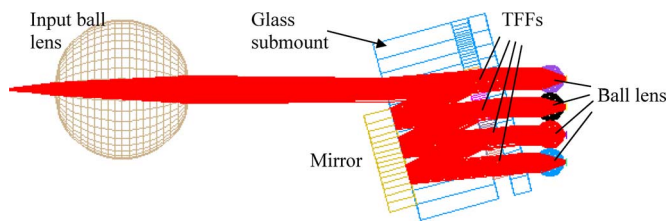


Fig. 9. Proposed hybrid glass submount SiOB.

IV. CONCLUSION

Optical sub-assembly (OSA) of DEMUX on SiOB was demonstrated using passive alignment approach. The design of the 4 channel MUX/DEMUX OSA using discrete TFFs assembled on a SiOB required very high assembly accuracy. The major challenge encountered for this design is to achieve a high perpendicularity for the mirror and TFF, estimated to be less than 0.3° . The measured coupling loss is higher than the simulation result because of the contribution from dimension error in x - and y -axis that caused the ball lenses misaligned to optical axial, curved bottom surface that led to large θ_x , and mostly the inherited inaccuracies of the optical devices. A cumulated coupling loss of 20.3 dB for SMF-SMF and 8.1 dB for SMF-MMF at channel 4 for an assembled DEMUX was achieved after controlling in adhesive volume, and pushing the optical devices as close as possible to the side wall. For the SiOB OSA to have a maximum coupling loss of less than 3 dB, the optical component used must have a tight control on the perpendicularity angle and the dimensions of the optical components (TFFs and mirror) and the SiOB cavities.

Another source of coupling loss is the ball lens misalignment. Unlike the TFF and mirror, this misalignment error is not cumulative for the subsequent channels. In theory, this ball lens misalignment can be solved using V-groove, which can help to ensure the ball lenses are located at the center optical path position. However, the V-groove design was not fabricated successfully in this work here. Instead, a flat bottom SiOB cavity fabricated using SOI wafer and a controlled perpendicularity mirror (dummy TFF) are used to quantify the assembly losses, i.e., ~ 16 dB for SMF and ~ 8 dB for MMF output coupling at channel 4. Mirrors with known θ_x were assembled into the SiOB with a relatively flat bottom surface to determine the effect of the inherited inaccuracies of optical devices to overall coupling loss. If the TFFs' and the mirror's tilting angles are identical, and are tilting at different direction, the misalignment

error could be compensated. However, it will be a challenge to control during assembly. The worst simulated scenario shows a coupling loss of infinity.

For future works, the design should utilize the front and back surfaces of TFFs and mirrors which is relatively flat and normal to optical axis for physical contact. An alternative solution is to utilize the hybrid glass submount SiOB structure as proposed during the development. The glass submount with one surface is coated to form a mirror and the opposite surface is used to assemble the TFF perpendicularly, while the SiOB is used to provide the ball lens assembly accuracy.

ACKNOWLEDGMENT

The authors would like to thank C. Teo, L. Lim, and E. Pa Pa for their technical support.

REFERENCES

- [1] S. H. Hwang, D. D. Seo, J. Y. An, M. H. Kim, W. C. Choi, S. R. Cho, S. H. Lee, H. H. Park, and H. S. Cho, "Parallel optical transmitter module using angled fibers and a V-grooved silicon optical bench for VCSEL array," *IEEE Trans. Adv. Packag.*, vol. 29, no. 3, pp. 457–462, Aug. 2006.
- [2] M. Pearson, S. Bidnyk, and A. Balakrishnan, "Hybridization of active and passive elements for planar photonic components and interconnects," in *Proc. Photonics Packag., Integration Interconnects VII*, A. M. Earman and R. T. Chen, Eds., 2007, vol. 6478, p. 64780L.
- [3] B. E. Lemoff, L. B. Aronson, and L. A. Buckman, "SpectraLAN: A low-cost multiwavelength local area network," *Hewlett-Packard J.*, pp. 42–52, Dec. 1997.
- [4] B. E. Lemoff, L. B. Aronson, and L. A. Buckman, "Zigzag waveguide demultiplexer for multimode WDM LAN," *Electron. Lett.*, vol. 34, pp. 1014–1016, 1998.
- [5] Y. Yamada, A. Sugita, K. Moriawaki, I. Ogawa, and T. Hashimoto, "An application of a silica-on-terraced-silicon platform to hybrid Mach-Zehnder interferometric circuits consisting of silica-waveguides and LiNbO₃ phase-shifters," *IEEE Photon. Technol. Lett.*, vol. 6, no. 7, pp. 822–824, 1994.
- [6] S. H. Hwang, J. Y. An, M. H. Kim, W. C. Choi, S. R. Cho, S. H. Lee, H. S. Cho, and H. H. Park, "VCSEL array module using (111) facet mirrors of a V-grooved silicon optical bench and angled fibers," *IEEE Photon. Technol. Lett.*, vol. 17, no. 2, pp. 477–479, 2005.
- [7] P. Schwab, T. Bowen, R. Perko, N. Delen, J. Goodrich, and R. Anderson, "A high throughput optoelectronic module assembly process," in *Proc. Electron. Compon. Technol. Conf.*, 2004, pp. 1475–1478.
- [8] J. T. Kim, K. B. Yoon, and C. G. Choi, "Passive alignment method of polymer PLC devices by using a hot embossing technique," *IEEE Photon. Technol. Lett.*, vol. 16, no. 7, pp. 1664–1666, Jul. 2004.
- [9] M. Li, H. K. Tsang, C. Shu, C. C. Wei, C. W. Law, Y. K. Lau, R. W. M. Kwok, X. W. Hu, and H. L. Zhu, "Photolithography of 3D topology in Si optical bench for self-aligned placement of laser dies," in *Proc. Electron. Compon. Technol. Conf.*, 2004, pp. 1925–1928.
- [10] M. F. Dautartas, J. Fisher, H. Luo, P. Datta, and A. Jeantilus, "Hybrid optical packaging, challenges & opportunity," in *Proc. Electron. Compon. Technol. Conf.*, 2002, pp. 787–793.

- [11] J. W. Osenbach, M. F. Dautartas, E. Pitman, C. Nijander, M. Brady, R. K. Schlenker, T. Butrie, S. P. Scrak, B. S. Auker, D. Kern, S. Salko, D. Rinaudo, C. Whitcraft, and J. F. Dormer, "Low cost/high volume laser modules using silicon optical bench technology," in *Proc. Electron. Compon. Technol. Conf.*, Seattle, WA, 1998, pp. 581–587.
- [12] R. Boudreau, P. Zhou, and T. Bowen, "Wafer scale photonic-die attachment," *IEEE Trans. Comp., Packag., Manuf. Technol. B*, vol. 21, no. 2, pp. 136–139, May 1998.



Chee-Wei Tan received the B.Sc. (Hon.) and M.Sc. degrees in materials science from the National University of Malaysia (UKM) and the Ph.D. degree in electronics engineering from City University of Hong Kong (CityUHK).

He is currently a Senior Research Engineer at the Institute of Microelectronics, Singapore. He is responsible for packaging of nano-photonics, especially silicon photonics. His research interests are photonics packaging and advanced packaging.



Teck-Guan Lim received the Diploma in electronics and communication engineering, and the Advanced Diploma in telecommunications from Singapore Polytechnic, the B.Eng. degree (First Class Honours) in electronic and electrical engineering, and the Ph.D. degree in microwave photonics engineering from the University of Surrey, U.K., in 1992, 1998, 2001, and 2005, respectively.

From 1992 to 1998, he served as an avionics specialist in the Republic of Singapore Air Force, specializing in electronic warfare. Currently, he is a Senior Research Engineer at the Microsystems, Modules and Components Laboratory, Institute of Microelectronics. He is responsible for the optical and electrical design for the packaging and is the group leader for the Electrical Design and Simulation team. His research interests include microwave and millimeter-wave integrated circuits.

Dr. Lim was awarded The Lord Lloyd of Kilgerran Memorial Prize, IET, U.K. (2002) for his postgraduate study.

Jing Li, photograph and biography not available at the time of publication.

Tangdionga Geri Endrio, photograph and biography not available at the time of publication.



Yi-Yoon Chai received the degree in electrical and electronics engineering from the National Technological University, Singapore, in 2005. She is currently working toward the M.Sc. degree in electrical engineering in the Department of Electrical and Computer Engineering, National University of Singapore (NUS).

She worked at the Institute of Microelectronics, Singapore, for three years as a Research Officer from 2006 to 2009. Her work involved design and characterization of optical transceivers and optical interconnects. She is currently working at the Nitto Denko Asia Technical Centre as a Research Engineer, working on optical coupling methods/structures and instrumentation for biomedical applications.



Seiji Maruo is currently with the Research & Development Group, Cross Technology Development Centre, Optical Interconnection Technology Unit, Hitachi Cable Ltd. He is working on the research and development of optical transceivers.



Pamidighantam V. Ramana received the M.S. degree in applied optics from the National Institute of Technology, Warangal, India, in 1984.

He has been a Member of Technical Staff (MTS) at the Institute of Microelectronics (IME), Singapore, since November 2001. He has over 23 years of experience in opto-electronics research and development in research institutes and multinational companies. His research interests include optical interconnects, optical imaging, illumination optics, and optical component packaging. Prior to joining

IME in 2001, he worked in the R&D Departments of Philips Optical Storage and Agilent Technologies. Before coming to Singapore, he was working in a military research institute with the Ministry of Defence, Government of India, on imaging and nonimaging optical guidance for missile systems. He has coauthored more than 50 research publications and has 10 invention disclosures in optics related products.



Seung-Wook Yoon (M'05) received the Ph.D. degree in materials science and engineering from the Korea Advanced Institute of Science and Technology (KAIST), Seoul, in 1998, and the M.B.A. degree from Nanyang Technology University, Singapore, in 2006.

He is Deputy Laboratory Director of Microsystem, Module, and Components (MMC) Laboratory, Institute of Microelectronics (IME), Singapore. His major interest fields are Cu/low-k/ultra low-k packaging, through silicon via (TSV) technology, 3-D silicon micromodule technology, wafer-level integration, and microsystem packaging. Prior to joining IME, he was a Member of the Technical Staff for Advanced Electronic Packaging and Memory Module Development, Hynix Semiconductor, in 1998. He worked for the development of lead-free solder applications, multichip packaging, CSP, wafer-level packaging, and was involved in JEDEC 11 activity. He is the author or coauthor of over 80 journal papers and conference papers and is the holder of several U.S. patents on microelectronic materials and electronic packaging.

Dr. Yoon is member of the TMS.



John H. Lau (M'88–SM'90–F'94) received three M.S. degrees in structural engineering, engineering physics, and management science, and the Ph.D. degree in theoretical and applied mechanics from the University of Illinois.

He has been a Professor at Hong Kong University Science and Technology (HKUST) since January 2009. Prior to that, he was the Director of Microsystems, Modules and Components (MMC) Laboratory with the Institute of Microelectronics (IME), Singapore, for two years and a Senior Scientist/SMTS at

HP/Agilent in the U.S. for more than 20 years. With more than 30 years of R&D and manufacturing experience, he has authored or coauthored more than 300 peer-reviewed technical publications and more than 100 book chapters, and given more than 250 presentations. He has authored and coauthored 16 textbooks on advanced packaging, solder joint reliability, and lead-free soldering and manufacturing.

Dr. Lau is an elected ASME Fellow and IEEE/CPMT Distinguished Lecturer.